The Impact of Bayesian Penalized Likelihood Reconstruction Algorithm on Quantitative Accuracy of Positron Emission Tomography Volumetric Measurements

Liang Chen
Zhejiang University School of Medicine Sir Run Run Shaw Hospital
Dongfang Chen
Xiasha Branch of Sir Run Run Shaw Hospital Affiliated to School of Medicine,Zhejiang University
Tao Huang
Zhejiang University School of Medicine Sir Run Run Shaw Hospital
Cen Lou (3194110@zju.edu)
Zhejiang University School of Medicine Sir Run Run Shaw Hospital

Original research

Keywords: Bayesian penalized likelihood, iterative adaptive, delineation method, metabolic tumor volume, phantom, PET

Posted Date: October 6th, 2020

DOI: https://doi.org/10.21203/rs.3.rs-68767/v1

Abstract

Objectives The metabolic tumor volume (MTV) of positron emission tomography/computed tomography (PET/CT) is an important index to evaluate the prognosis and the responses of treatments. The purpose of this study is to assess the impact of Bayesian Penalized Likelihood (BPL) reconstruction algorithm and segmentation methods on the accuracy of MTV via a phantom study.

Methods Using the National Electrical Manufactures Association/International Electrotechnical Commission (NEMA/IEC) image quality phantom, six hot spheres and background were filled with 21.56 KBq/ml and 5.39 KBq/ml Na 18 F (a sphere to background ratio of 4: 1). Acquired images were reconstructed using BPL (β = 400) and non-BPL (Ordered subsets expectation maximization + time of flight + point spread function, OSEM+TOF+PSF) algorithms, respectively. MTVs of six spheres were delineated using maximum standardized uptake value (SUV max) percentage threshold method and iterative adaptive method, respectively. The actual measured volumes of spheres were used as the standard for comparative analysis.

Results The MTVs measurement errors in BPL were 4.96%, -3.00%, 6.18%, 5.20%, -10.00% and 18.33%, which was significantly lower than that in non-BPL (Z = - 2.562, p = 0.009), and the measurement errors in non-BPL were 16.70%, 10.77%, 26.00%, 30.00%, 61.82% and 113.33%. The optimal percentage SUV max threshold of spheres in BPL algorithm was raged in 40% - 45%, which was not affected by the ball size. And there was no significant difference of MTVs measurement accuracy between the 42%SUV max and iterative adaptive threshold (Z = -0.48, p = 0.699). However, using the non-BPL algorithm, the measurement errors of 42%SUV max and iterative adaptive delineation methods were 16.70%, 10.77%, 26.00%, 30.00%, 61.82%, 113.33%, and -7.70%, -9.00%, -8.73%, -5.20%, -12.91%, 38.33% respectively. The MTVs measurement accuracy of iterative adaptive was significantly better than that of the 42%SUV max threshold (Z = -2.24, p = 0.026). The iterative adaptive and 42%SUV max threshold methods had excellent interobserver reliability (ICCs=1.00 for all of six spheres) for MTVs measurement.

Conclusion BPL reconstruction algorithm can improve the accuracy of MTVs measurements, especially for small lesions. In the case of using non-BPL methods, the iterative adaptive delineation method should be adopted to improve the accuracy of MTVs measurements.

Introduction

The quantitative parameters of PET/CT have been widely used in tumor clinical practice. In addition to uptake metabolic parameters such as SUV_{max} and SUV_{mean}, volume metabolic parameters MTV and total lesion glycolysis (TLG, defined as MTV × SUV_{mean}) are also becoming more and more important. Studies have shown that MTV and TLG are closely related to tumor burden, treatment response evaluation and prognosis judgment [1–5]. Consequently, accurate MTV measurements of tumor lesions have become a challenge for achieving clinical purposes. In addition, the accuracy of MTV measurement highly depends on the PET/CT image reconstruction method and lesion delineation method.

Bayesian penalized likelihood (BPL) reconstruction is a new PET/CT reconstruction algorithm based on the iterative reconstruction [6]. Compared with conventional reconstruction methods, BPL does not only improve the quantitation accuracy of lesions, but also effectively reduce the noise level of the image, and then improve the general image quality and conspicuity of small lesions [7]. However, the method using for MTV delineation also needs to be careful and precise. At present, most studies use a fixed SUV threshold (such as SUV ≥ 2.5 or SUV ≥ 4.0) or a percentage of SUV_{max} (such as 42% SUV_{max}) to define MTV [8–10]. Meanwhile, Xu et al. also proposed that using the iterative adaptive method of PET VCAR software (GE Healthcare, Milwaukee) was more accurate than using the SUV_{max} percentage threshold method to determine MTVs [11].

According to literatures, there are few studies on how different image reconstruction methods and MTV delineation methods affects the accuracy of the MTV measurement, and how to effectively combine reconstruction algorithms with delineation methods to further improve the accuracy of MTV measurement. Therefore, this study performed a phantom study to analyze the impact of BPL reconstruction algorithm and delineation methods on the accuracy of the MTV measurement.

Methods

Phantom image acquisition and reconstruction

A NEMA/IEC image quality phantom (CAPINTEC,INC, USA) was used, in which 6 spheres (D = 37 mm, 28 mm, 22 mm, 17 mm, 13 mm and 10 mm) were filled with 21.56 KBq/ml of $Na^{18}F$ while the background concentration was 5.39 KBq/ml, with sphere-to-background activity ratio of 4 : 1. $Na^{18}F$ was provided by Shanghai Atom Kexing Pharmaceuticals Co.,LTD with radiochemical purity > 99%. A GE Discovery MI PET/CT (DMI, GE Healthcare, Milwaukee) was used to perform scans with PET acquisition parameters: 3 min/bed, slice thickness 3.75 mm, matrix 256 × 256. CT acquisition parameters: tube voltage 120 kv, auto mA(60-150mA), noise index 25, pitch 0.984, slice thickness 3.75 mm, rotation time 0.5 s. Two different iterative reconstruction algorithms were used for reconstruction, namely BPL (Ordered subsets expectation maximization + time of flight + point spread function +BPL, with a noise suppression factor, β, of 400) and non-BPL (conventional OSEM + TOF + PSF, 3 iterations, 16 subsets and 6.4mm Gaussian filter).

Image analysis

The AW workstation (GE Healthcare, Milwaukee) was used for image fusion and processing. The PET VCAR software (GE Healthcare, Milwaukee) was used to reconstruct PET images with BPL and non-BPL methods respectively. The volume of interest (VOI) was delineated on six hot spheres by using three different methods: the SUV_{max} percentage threshold method (range: 30% - 70%, with an increasement of 5%); the 42%SUV_{max} threshold method; the iterative adaptive

method. The MTV values (cm^3) were then calculated automatically. In iterative adaptive method, SUV_{max} and SUV_{mean} were weighted by a weighting factor to determine the delineation threshold of the VOI and background tissue, which was automatically set to 0.5 [12].

By using BPL and non-BPL reconstruction methods, three experienced nuclear medicine physicians used the percentage SUV_{max} threshold method and the iterative adaptive method to delineate VOIs and recorded MTV readings of each hot sphere. For VOIs delineation, a boundary box (i.e. the tool for automatic delineation and segmentation of VOIs) was placed on the PET image at the lesion layer. The cross-sectional, coronal and sagittal sections were repeatedly checked and adjusted to ensure that the whole hot sphere was included and the background was excluded.

Pure water was injected into each sphere manually to determine the actual volumes of spheres, which were then used as the gold standard. The percentage errors between MTVs and actual volumes (%error = (MTV – actual volume) x 100% / actual volume) were then calculated to determine the optimal $\%SUV_{max}$ threshold and the best delineation methods under different reconstruction methods. Results with the smallest %error were considered as the best option.

Statistical analysis

All data were analyzed by using the SPSS 22.0 software. Mann-Whitney U test was used to compare the MTVs errors of different reconstruction methods and different delineation methods. The intraclass correlation coefficient (ICC) was used to estimate the measurement reliability of MTVs using the 42% SUV_{max} and the iterative adaptive methods. Results were considered as statistically significant when $p < 0.05$.

Results

Figure 1 shows the PET/CT transversal images of the phantom with six hot spheres were clearly displayed without deformation under the BPL reconstruction method, especially the image clarity and edge sharpness of 13 mm and 10 mm spheres were significantly better than those of non-BPL images. By using the $42\%SUV_{max}$ threshold as the delineation method, results showed that the measurement errors of MTVs in BPL were 4.96%, -3.00%, 6.18%, 5.20%, -10.00% and 18.33%, which was significantly lower than that in non-BPL ($Z = -2.562$, $p = 0.009$), and the measurement errors in non-BPL were 16.70%, 10.77%, 26.00%, 30.00%, 61.82% and 113.33% (Table 1).

Table 1
,Comparison of spheres MTV measurement accuracy between BPL and non-BPL reconstruction algorithms

Spheres	Actual volume (cm^3)	MTV (cm^3)		Errors%	
		BPL	non-BPL	BPL	non-BPL
37 mm	27	28.34	31.51	5.00%	17.00%
28 mm	13	12.61	14.4	-3.00%	11.00%
22 mm	5.5	5.84	6.93	6.00%	26.00%
17 mm	2.5	2.63	3.25	5.00%	30.00%
13 mm	1.1	0.99	1.78	-10.00%	62.00%
10 mm	0.6	0.71	1.28	18.00%	113.00%
The errors of spheres MTVs in BPL were significantly lower than non-BPL algorithm (Mann-Whitney U, Z=-2.562, p = 0.009) by $42\%SUV_{max}$ threshold delineation method, and BPL algorithm especially improved the accuracy of the smaller spheres MTV (13 mm and 10 mm).					

Taking actual volumes of hot spheres as the gold standard (Table 2), the optimal percentage SUV_{max} threshold of all hot spheres under BPL reconstruction was raged in 40% – 45%, which was not affected by the ball size. However, the optimal threshold percentage range was 45% – 60% under non-BPL reconstruction, and the smaller spheres (13 mm and 10 mm) needed to increase the threshold% to improve the accuracy of MTVs measurements.

Table 2

,Comparison of spheres MTVs (cm^3) and optimal threshold% in BPL and non-BPL reconstruction algorithms.

Spheres	Actual volume	30%SUV_{max}	35%SUV_{max}	40%SUV_{max}	45%SUV_{max}	50%SUV_{max}	55%SUV_{max}	60%SUV_{max}	65%SUV_{max}	70%SUV_{ma}
MTV-BPL (cm^3)										
37 mm	27	35.42 ± 0.57	31.76 ± 0.79	29.19 ± 2.01	27.38 ± 1.4	25.67 ± 2.31	24.04 ± 2.01	22.82 ± 2.02	21.40 ± 1.54	19.85 ± 1.51
28 mm	13	17.34 ± 1.30	14.26 ± 1.20	13.26 ± 1.61	11.99 ± 1.60	11.26 ± 1.08	10.37 ± 0.56	9.49 ± 1.46	8.87 ± 1.10	8.07 ± 0.19
22 mm	5.5	8.5 ± 0.59	7.26 ± 0.50	6.14 ± 0.17	5.51 ± 1.71	4.92 ± 0.56	4.44 ± 0.54	4.08 ± 0.23	3.64 ± 0.45	3.16 ± 0.29
17 mm	2.5	4.24 ± 0.17	3.29 ± 0.08	2.80 ± 0.22	2.49 ± 0.19	2.12 ± 0.16	1.62 ± 0.38	1.49 ± 0.23	1.37 ± 0.15	1.18 ± 0.14
13 mm	1.1	1.83 ± 0.15	1.32 ± 0.25	1.10 ± 0.11	0.89 ± 0.11	0.71 ± 0.11	0.56 ± 0.05	0.47 ± 0.13	0.38 ± 0.06	0.31 ± 0.02
10 mm	0.6	1.46 ± 0.38	1.11 ± 0.32	0.86 ± 0.32	0.59 ± 0.40	0.47 ± 0.26	0.36 ± 0.26	0.30 ± 0.19	0.22 ± 0.12	0.17 ± 0.11
MTV-non-BPL(cm^3)										
37 mm	27	41.92 ± 1.75	36.10 ± 3.74	32.5 ± 2.47	29.57 ± 2.89	27.17 ± 1.86	24.85 ± 2.04	22.87 ± 3.01	20.73 ± 2.09	18.84 ± 1.97
28 mm	13	21.48 ± 1.32	17.61 ± 1.24	15.05 ± 1.01	13.23 ± 1.11	11.81 ± 2.17	10.50 ± 0.65	9.33 ± 0.67	8.36 ± 0.26	7.24 ± 0.41
22 mm	5.5	10.81 ± 1.02	8.62 ± 1.36	7.25 ± 0.37	6.26 ± 0.59	5.47 ± 0.36	4.65 ± 0.33	4.04 ± 1.40	3.36 ± 0.27	2.85 ± 0.51
17 mm	2.5	5.35 ± 1.04	4.34 ± 1.33	3.54 ± 0.33	2.82 ± 0.47	2.49 ± 0.65	1.87 ± 0.92	1.49 ± 0.73	1.30 ± 0.78	1.06 ± 0.87
13 mm	1.1	4.16 ± 1.23	2.61 ± 1.1	1.92 ± 0.98	1.50 ± 0.97	1.36 ± 0.67	0.98 ± 0.65	0.67 ± 0.27	0.45 ± 0.32	0.36 ± 0.26
10 mm	0.6	4.14 ± 2.96	4.08 ± 1.65	2.53 ± 1.27	1.59 ± 0.95	1.16 ± 0.85	0.83 ± 0.26	0.63 ± 0.09	0.47 ± 0.11	0.32 ± 0.09

Table 3 and Fig. 2 show that, by using the BPL reconstruction method, the MTVs measurement errors of 42%SUV_{max} and iterative adaptive methods were 4.96%, -3.00%, 6.18%, 5.20%, -10.00%, 18.33% and − 3.22%, -7.92%, 5.82%, 9.20%, 11.82%, 15.00%, There was no significant difference between the two methods (Z = -0.48, p = 0.699). However, using the non-BPL reconstruction, the errors of iterative adaptive method and 42%SUV_{max} method were-7.70%, -9.00%, -8.73%, -5.20%, -12.91%, 38.33% and 16.70%, 10.77%, 26.00%, 30.00%, 61.82%, 113.33%, respectively. The MTVs measurement accuracy of iterative adaptive method was significantly better than that of the 42%SUV_{max} threshold (Z = -2.24, p = 0.026).

Table 3

, The impact of BPL reconstruction algorithm and delineation method on MTV measurement accuracy

Spheres	Actual volume (cm^3)	MTV-BPL (cm^3)		MTV-Non-BPL (cm^3)		Errors% in BPL		Errors% in non-BPL	
		42%SUV_{max}	Iterative	42%SUV_{max}	Iterative	42%SUV_{max}	Iterative	42%SUV_{max}	Iterative
37 mm	27	28.34	26.13	31.51	24.92	4.96%	-3.22%	16.70%	-7.70%
28 mm	13	12.61	11.97	14.4	11.83	-3.00%	-7.92%	10.77%	-9.00%
22 mm	5.5	5.84	5.82	6.93	5.02	6.18%	5.82%	26.00%	-8.73%
17 mm	2.5	2.63	2.73	3.25	2.37	5.20%	9.20%	30.00%	-5.20%
13 mm	1.1	0.99	1.23	1.78	0.958	-10.00%	11.82%	61.82%	-12.91%
10 mm	0.6	0.71	0.69	1.28	0.83	18.33%	15.00%	113.33%	38.33%
In BPL, there was no significant difference in MTV measurement accuracy by 42%SUVmax and iterative adaptive threshold methods (Mann-Whitney U, Z=-0.48, p = 0.699). In non-BPL, the errors% of MTVs measurement by iterative adaptive were significantly lower than 42%SUVmax threshold delineation method (Mann-Whitney U, Z=-2.24, P = 0.026).									

The ICC of the iterative adaptive and the 42%SUV_{max} threshold methods were 1.00 (95% CI: 1.00 ~ 1.00), 1.00 (95% CI: 1.00 ~ 1.00), 1.00 (95% CI: 1.00 ~ 1.00), 1.00 (95% CI: 1.00 ~ 1.00), 1.00 (95% CI: 0.99 ~ 1.00) for six spheres, respectively. These two methods showed excellent reliability and very high measurement consistency.

Discussion

A number of studies have consistently shown that MTV of PET/CT can provide valuable diagnostic and prognostic information for malignant tumors, and can be used to monitor disease progression and evaluate treatment response [3, 4]. In addition, PET/CT has been proved to be very important for defining the target volume of radiotherapy. The precise definition of MTV is essential for increasing the radiation dose of pancreatic cancer, gynecological tumor and rectal

cancer, reducing the risk of organ exposure, and developing personalized *in vitro* radiotherapy plan [13, 14]. PET quantitative accuracy is affected not only by the hardware of equipment, but also by reconstruction algorithms. The BPL reconstruction method is the latest commercial PET/CT reconstruction algorithm which can be used in clinic. In novel PET/CT imaging systems, BPL is allowed to be applied simultaneously with TOF and PSF, results in significant improvements in signal-to-noise ratio, contrast and reconstruction resolution while keeping the edge unchanged and better quantitation accuracy compared with conventional reconstruction methods [15].

In this study, the actual volumes of NEMA phantom spheres were used as the reference, and the BPL reconstruction algorithm significantly improved the measurement accuracy of MTV compared with the non-BPL reconstruction algorithm. BPL significantly reduced the MTV measurement error when using the 42%SUV_{max} threshold delineation method ($p = 0.009$). Parvizin et al. [16] carried out a study on PET/CT quantitative parameters of 42 liver metastases (mean diameter of 25 mm, range of 6–86 mm). Using 40%SUV_{max} as the threshold, the MTVs of lesions decreased from 21.5 ml (1.5–143.4 ml) of OSEM to 16.3 ml (0.7–110.4 ml) of BPL ($p < 0.001$). According to Vallot D et al. [6], the MTV of 61.8% tumor lesions in BPL group was lower than that in OSEM group, but the difference was not significant ($p = 0.069$). This result is attributed to the full convergence of BPL reconstruction algorithm. Compared with conventional OSEM methods, BPL can reduce the noise and increase the number of iterations. By regularizing the relative difference between adjacent pixels of β parameter penalized, the image presents the optimal contrast and reconstruction resolution while maintaining the edge of the lesion, so as to ensure the accuracy of MTV. In addition, the accuracy of the 42%SUV_{max} threshold method mostly depends on the accuracy of SUV_{max}. Phantom and clinical case studies have confirmed the role of BPL algorithm in accurate quantification of SUV_{max}, and this improvement is mainly focused on small lesions [17]. Results shown in Table 1 are consistent with their findings, which show that BPL can significantly reduce the MTV measurement errors of 13 mm and 10 mm spheres. At the same time, the role of BPL algorithm to keep the lesion edge unchanged also avoids the Gibbs artifact of small lesion edge given from PSF [18, 19]. Therefore, compared with the non-BPL algorithm, the BPL algorithm obtains higher reconstruction spatial resolution [20], reduces the impact of partial volume effect on small lesions, and improves the quantitative accuracy of MTV for small lesions.

The latest research of Texte E et al. also proposed that BPL reconstruction method can significantly reduce the MTV of lung tumor lesions, and results are also closely related to the delineation method of tumor lesions [21]. In this study, the incremental% SUV_{max} threshold was used to find the optimal delineation threshold of the BPL and non-BPL methods. The results showed that the optimal segmentation threshold under BPL was fall in a relatively narrower range of 40% − 45%, when compared with the non-BPL group (45% − 60%). Notably, the segmentation threshold of small lesions needed to be adjusted to 60% to achieve acceptable MTV errors when using the non-BPL method. That is to say, under the BPL reconstruction method, the manufacturer's default setting of 42% can meet the acceptable MTV accuracy of any size lesions. This further avoids the error caused by manual adjustment of thresholds and increases the results repeatability.

The results also showed that, by using the BPL method, the MTV error range of the 42%SUV_{max} and the iterative adaptive methods are − 3.00% ~ 18.33% and − 3.22% ~ 15.00% (from 37 mm to 10 mm), respectively, and there was no significant difference between them ($p = 0.699$). It indicates that BPL algorithm can make the measurement less affected by the segmentation method. With the non-BPL reconstruction method, PET/CT quantitative studies on cervical cancer and lung cancer lesions have confirmed that the iterative adaptive method can improve the MTV measurement accuracy [10, 11]. The iterative adaptive method is to get the optimal threshold value by weighting SUV_{max} and SUV_{mean} in the targeted lesion [12]. This means that MTV measured by the iterative adaptive method is determined by SUV_{max} and SUV_{mean} at the same time. This is more accurate than that of percentage SUV_{max} threshold method, which is only determined by SUV_{max}. Therefore, in view of the performance advantages of BPL reconstruction algorithm combined with iterative adaptive delineation methods the results of this study have guiding value for clinical practice of quantitative accuracy of PET/CT volumetric measures.

In this study, we did not study the effect of BPL on the accuracy of MTV measurement of actual tumor lesions. The research of NEMA phantom was carried out under the ideal conditions of regular shape and uniform radioactive distribution, the impact of BPL on MTV measurement accuracy of tumor lesions with irregular edge and heterogeneous radioactive uptake may be different. In addition, the sphere-to-background ratio was 4: 1 in this study, the results of different sphere-to-background ratios need to be further investigated by relevant phantom and clinical studies.

Conclusion

The BPL reconstruction algorithm can significantly improve the accuracy of MTV measurement, especially for small lesions. With the non-BPL reconstruction algorithm, the accuracy of MTV measurement can also be improved by using the iterative adaptive segmentation method.

Declarations

Compliance with Ethical Standards

The authors declare that have no conflict of interest. This paper does not contain any studies with human participants performed by any of the authors. For this type of study formal consent is not required.

Acknowledgement

None

References

1. Castello A, Rossi S, Mazziotti E, Toschi L, Lopci E. Hyperprogressive Disease in Patients with Non-Small Cell Lung Cancer Treated with Checkpoint Inhibitors: The Role of ^{18}F-FDG PET/CT. J Nucl Med. 2020;61(6):821–6. doi:10.2967/jnumed.119.237768.
2. Berriolo-Riedinger A, Becker S, Casasnovas O, Vander Borght T, Édeline V. Role of FDG PET-CT in the treatment management of Hodgkin lymphoma. Cancer Radiother. 2018;22(5):393–400. doi:10.1016/j.canrad.2018.06.001.
3. Monterisi S, Castello A, Toschi L, et al. Preliminary data on circulating tumor cells in metastatic NSCLC patients candidate to immunotherapy. Am J Nucl Med Mol Imaging. 2019;9(6):282–95. Published 2019 Dec 15.
4. Fasmer KE, Gulati A, Dybvik JA, et al. Preoperative 18F-FDG PET/CT tumor markers outperform MRI-based markers for the prediction of lymph node metastases in primary endometrial cancer. Eur Radiol. 2020;30(5):2443–53. doi:10.1007/s00330-019-06622-w.
5. Zhang H, Wroblewski K, Liao S, et al. Prognostic value of metabolic tumor burden from (18)F-FDG PET in surgical patients with non-small-cell lung cancer. Acad Radiol. 2013;20(1):32–40. doi:10.1016/j.acra.2012.07.002.
6. Vallot D, Caselles O, Chaltiel L, et al. A clinical evaluation of the impact of the Bayesian penalized likelihood reconstruction algorithm on PET FDG metrics. Nucl Med Commun. 2017;38(11):979–84. doi:10.1097/MNM.0000000000000729.
7. Miwa K, Wagatsuma K, Nemoto R, et al. Detection of sub-centimeter lesions using digital TOF-PET/CT system combined with Bayesian penalized likelihood reconstruction algorithm [published online ahead of print, 2020 Jul 4]. Ann Nucl Med. 2020. 10.1007/s12149-020-01500-8. doi:10.1007/s12149-020-01500-8.
8. Burggraaff CN, Rahman F, Kaßner I, et al. Optimizing Workflows for Fast and Reliable Metabolic Tumor Volume Measurements in Diffuse Large B Cell Lymphoma. Mol Imaging Biol. 2020;22(4):1102–10. doi:10.1007/s11307-020-01474-z.
9. Grozdic Milojevic I, Tadic M, Sobic-Saranovic D, Saponjski J, Artiko VM. Hybrid Imaging in Head and Neck Sarcoidosis. J Clin Med. 2019;8(6):803. Published 2019 Jun 5. doi:10.3390/jcm8060803.
10. Wang XY, Zhao YF, Liu Y, Yang YK, Zhu Z, Wu N. Comparison of different automated lesion delineation methods for metabolic tumor volume of 18F-FDG PET/CT in patients with stage I lung adenocarcinoma. Medicine. 2017;96(51):e9365. doi:10.1097/MD.0000000000009365.
11. Xu W, Yu S, Ma Y, Liu C, Xin J. Effect of different segmentation algorithms on metabolic tumor volume measured on 18F-FDG PET/CT of cervical primary squamous cell carcinoma. Nucl Med Commun. 2017;38(3):259–65. doi:10.1097/MNM.0000000000000641.
12. Moule RN, Kayani I, Prior T, et al. Adaptive 18fluoro-2-deoxyglucose positron emission tomography/computed tomography-based target volume delineation in radiotherapy planning of head and neck cancer. Clin Oncol (R Coll Radiol). 2011;23(5):364–71. doi:10.1016/j.clon.2010.11.001.
13. Fiorentino A, Laudicella R, Ciurlia E, et al. Positron emission tomography with computed tomography imaging (PET/CT) for the radiotherapy planning definition of the biological target volume: PART 2. *Crit Rev Oncol Hematol*. 2019;139:117–124. doi:10.1016/j.critrevonc. 2019.03.008.
14. Onal C, Torun N, Akyol F, et al. Integration of 68 Ga-PSMA-PET/CT in Radiotherapy Planning for Prostate Cancer Patients. Clin Nucl Med. 2019;44(9):e510–6. doi:10.1097/RLU.0000000000002691.
15. Ahn S, Fessler JA. Globally convergent image reconstruction for emission tomography using relaxed ordered subsets algorithms. IEEE Trans Med Imaging. 2003;22(5):613–26. doi:10.1109/TMI.2003.812251.
16. Parvizi N, Franklin JM, McGowan DR, Teoh EJ, Bradley KM, Gleeson FV. Does a novel penalized likelihood reconstruction of 18F-FDG PET-CT improve signal-to-background in colorectal liver metastases? Eur J Radiol. 2015;84(10):1873–8. doi:10.1016/j.ejrad.2015.06.025.
17. Teoh EJ, McGowan DR, Bradley KM, Belcher E, Black E, Gleeson FV. Novel penalised likelihood reconstruction of PET in the assessment of histologically verified small pulmonary nodules. Eur Radiol. 2016;26(2):576–84. doi:10.1007/s00330-015-3832-y.
18. Kidera D, Kihara K, Akamatsu G, et al. The edge artifact in the point-spread function-based PET reconstruction at different sphere-to-background ratios of radioactivity. Ann Nucl Med. 2016;30(2):97–103. doi:10.1007/s12149-015-1036-9.
19. Yamaguchi S, Wagatsuma K, Miwa K, Ishii K, Inoue K, Fukushi M. Bayesian penalized-likelihood reconstruction algorithm suppresses edge artifacts in PET reconstruction based on point-spread-function. Phys Med. 2018;47:73–9. doi:10.1016/j.ejmp.2018.02.013.
20. Rogasch JM, Suleiman S, Hofheinz F, et al. Reconstructed spatial resolution and contrast recovery with Bayesian penalized likelihood reconstruction (Q.Clear) for FDG-PET compared to time-of-flight (TOF) with point spread function (PSF). *EJNMMI Phys*. 2020;7(1):2. Published 2020 Jan 10. doi:10.1186/s40658-020-0270-y.
21. Texte E, Gouel P, Thureau S, et al. Impact of the Bayesian penalized likelihood algorithm (Q.Clear®) in comparison with the OSEM reconstruction on low contrast PET hypoxic images. *EJNMMI Phys*. 2020;7(1):28. Published 2020 May 12. doi:10.1186/s40658-020-00300-3.

Figures

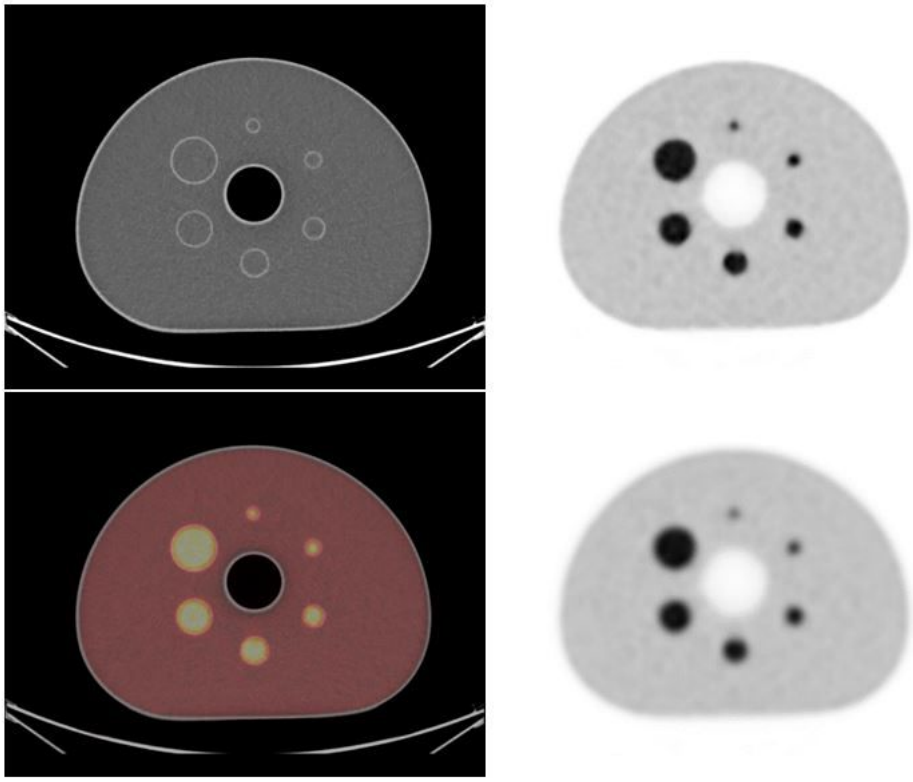

Figure 1

PET/CT images of NEMA/IEC phantom with BPL and non-BPL reconstruction algorithm. Spheres-to-background Na18F activity ratio was 4:1. The upper left, lower left, upper right and lower right images were CT, PET/CT fusion, BPL-PET and non-BPL-PET transversal images.

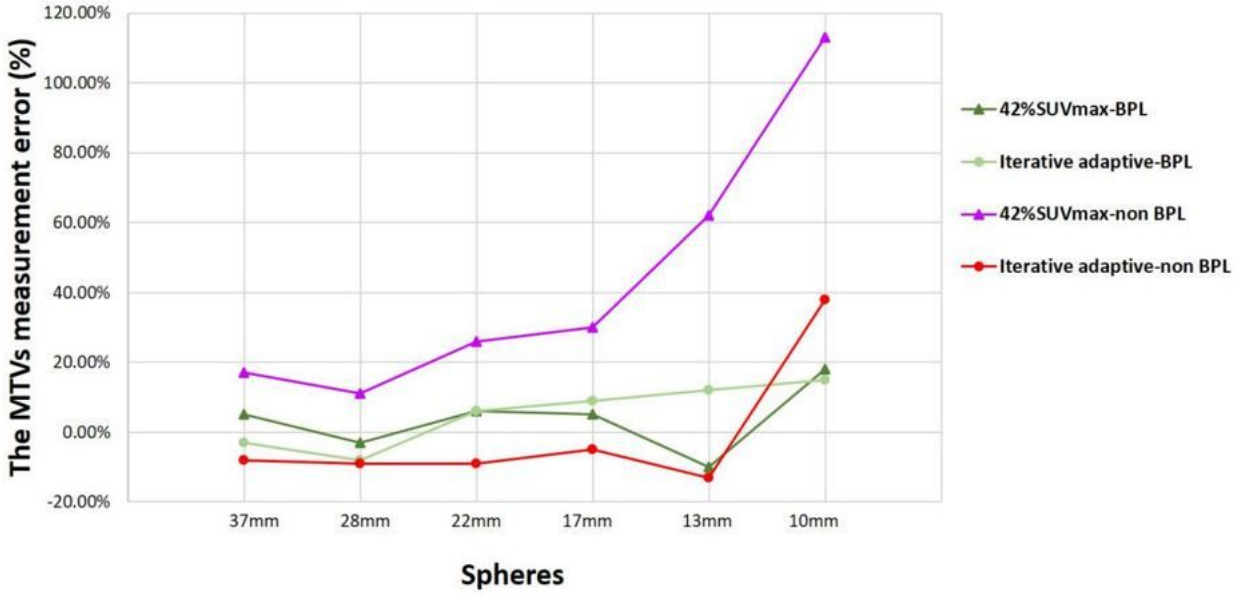

Figure 2

The impact of PET reconstruction algorithm and six spheres delineation method on MTV measurement accuracy in phantom (sphere-to-background ratio of 4:1)